Systematic Crystallographic Investigation of Hydrogen-Bonded Networks Involving Monohydrogen Tartrate−Amine Complexes: Potential Materials for Nonlinear Optics[||]

Renuka Kadirvelraj,[†] Arun M. Umarji,[‡] Ward T. Robinson,[§] Santanu Bhattacharya,[⊥] and Tayur N. Guru Row*[,†,⊥]

Solid State and Structural Chemistry Unit, Materials Research Centre, and Department of Organic Chemistry, Indian Institute of Science, Bangalore 560012, India, and Department of Chemistry, University of Canterbury, Private bag 4800, Christchurch, New Zealand

Received February 12, 1996. Revised Manuscript Received May 17, 1996[⊗]

Crystal structures of six binary salts involving aromatic amines as cations and hydrogen tartrates as anions are presented. The materials are 2,6-xylidinium-L-monohydrogen tartrate monohydrate, $C_{12}H_{18}O_{6.5}N$, $P22_12_1$, $a = 7.283(2)$ Å, $b = 17.030(2)$ Å, $c = 22.196(2)$ Å, $Z = 8$; 2,6-xylidinium-D-dibenzoyl monohydrogen tartrate, $C_{26}H_{25}O_8N$, $P2_1$, $a = 7.906(1)$ Å, $b = 24.757(1)$ Å, $c = 13.166(1)$ Å, $\beta = 105.01(1)°$, $Z = 4$; 2,3-xylidinium-D-dibenzoyl monohydrogen tartrate monohydrate, $C_{26}H_{26}O_{8.5}N$, $P2_1$, $a = 7.837(1)$ Å, $b = 24.488(1)$ Å, $c = 13.763(1)$ Å, $\beta = 105.69(1)°$, $Z = 4$; 2-toluidinium-D-dibenzoyl monohydrogen tartrate, $C_{25}H_{23}O_8N$, $P2_12_12_1$, $a = 13.553(2)$ Å, $b = 15.869(3)$ Å, $c = 22.123(2)$ Å, $Z = 8$; 3-toluidinium-D-dibenzoyl monohydrogen tartrate (1:1), $C_{25}H_{23}O_8N$, $P1$, $a = 7.916(3)$ Å, $b = 11.467(6)$ Å, $c = 14.203(8)$ Å, $\alpha = 96.44(4)°$, $\beta = 98.20(5)°$, $= 110.55(5)°$, $Z = 2$; 3-toluidinium-D-dibenzoyl tartrate dihydrate (1:2), $C_{32}H_{36}O_{10}N$, $P1$, $a = 7.828(3)$ Å, $b = 8.233(1)$ Å, $c = 24.888(8)$ Å, $\alpha = 93.98°$, $\beta = 94.58(3)°$, $= 89.99(2)°$, $Z = 2$. An analysis of the hydrogen-bonding schemes in terms of crystal packing, stoichiometric variations, and substitutional variations in these materials provides insights to design hydrogen-bonded networks directed toward the engineering of crystalline nonlinear optical materials.

Introduction

The assembly of organic molecules in crystal structures is mainly dependent on intermolecular interactions[1] and a careful understanding of crystal packing forces such as electrostatic, hydrogen bond, van der Waals, and stacking interactions form the basis of crystal engineering.[2] The use of hydrogen bonding between molecular entities is by far the most convenient way to employ among these interactions in directing the molecular self-assembly.[3] To design crystalline solids with desired properties, a complete knowledge of the features of hydrogen bonding becomes essential.[4] The design of new solid-state materials has led to the synthesis of well-organized aggregates involving hydrogen bonding[5] and extended structures with predictable backbones directed by hydrogen bonds.[6] Hydrogen-bonded anionic structures with suitable frameworks for polarizable cations[7] are also novel materials for nonlinear optics. For example, a recent study on hydrogen malate anions has illustrated that these anions may be utilized as building blocks to generate two-dimensional structural frameworks wherein cations of desired dimensions could be incorporated for generating specific properties.[7b] The use of hydrogen bonding as an adhesive force has been exploited in several classes of compounds such as carboxylic acids,[7,8] nitroanilines,[9] dihydrogen phosphates,[10] hydrogen sulfates,[11] diaryl ureas,[12] imides,[13] and guanidinium sulfonates.[14] Hydrogen-bonding networks have also been used to design

[†] Solid State and Structural Chemistry Unit.
[‡] Materials Research Centre.
[§] University of Canterbury.
[⊥] Department of Organic Chemistry.
* To whom correspondence should be addressed.
[||] Contribution No. 1107 from Solid State and Structural Chemistry Unit, Indian Institute of Science, Bangalore 560012, India.
[⊗] Abstract published in *Advance ACS Abstracts,* July 1, 1996.

(1) Warshel, A.; Lifson, S. *J. Chem. Phys.* **1970**, 582.
(2) (a) Whitesides, G. M.; Simanek, E. E.; Mathias, J. P.; Seto, C. T.; Chin, D. N.; Mammen, M.; Gordon, D. M. *Acc. Chem. Res.* **1995**, *28*, 37 and references therein. (b) Lehn, J.-M. *Science* **1993**, *260*, 1762 and references therein. (c) Lehn, J.-M. *Top. Curr. Chem.* **1993**, 165 and articles therein. (d) Mathias, J. P.; Stoddart, J. F. *Chem. Soc. Rev.* **1992**, *21*, 215 and references therein. (e) *Crystal Engineering: The design of organic solids*; Desiraju, G. R., Ed.; Elsevier: Amsterdam, 1989. (g) Lehn, J.-M. *Angew. Chem., Int. Ed. Engl.* **1988**, *27*, 89 and references therein.
(3) (a) Macdonald, J. C.; Whitesides, G. M. *Chem. Rev.* **1994**, *94*, 2383 and references therein. (b) Zerkowski, J. A.; Whitesides, G. M. *J. Am. Chem. Soc.* **1994**, *116*, 4298. (c) Fan, E.; Vincent, C.; Geib, S. J.; Hamilton, A. D. *Chem. Mater.* **1994**, *6*, 1113 and references therein. (d) Seto, C. T.; Whitesides, G. M. *J. Am. Chem. Soc.* **1993**, *115*, 905. (e) Geib, S. J.; Vincent, C.; Fan, E.; Hamilton, A. D. *Angew. Chem., Int. Ed. Engl.* **1993**, *32*, 119 and references therein. (f) Yang, J.; Fan, E.; Geib, S.; Hamilton, A. D. *J. Am. Chem. Soc.* **1993**, *115*, 5314. (g) Zimmerman, S. C.; Duerr, B. F. *J. Org. Chem.* **1992**, *57*, 2215. (h) Lindsey, J. S. *New J. Chem.* **1991**, *15*, 153. (i) Lehn, J.-M. *Angew Chem., Int. Ed. Engl.* **1990**, *29*, 1304.
(4) (a) Bernstein, J.; Davis, R. E.; Shimoni, L.; Chang, N.-L. *Angew. Chem., Int. Ed. Engl.* **1995**, *34*, 1555 and references therein. (b) Etter, M. C.; Reutzel, S. M.; Choo, C. G. *J. Am. Chem. Soc.* **1993**, *115*, 4411 and references therein. (c) Aakeroy, C. B.; Seddon, K. R. *Chem. Soc. Rev.* **1993**, 397. (d) Reutzel, S. M.; Etter, M. C. *J. Phys. Org. Chem.* **1992**, *5*, 44 and references therein. (e) Etter, M. C. *J. Phys. Chem.* **1991**, *95*, 4601. (f) *The Hydrogen Bond: Recent Developments in Theory and Experiments*; Schuster, D., Zundel, G., Zandorfy, C., Eds.; North Holland: Amsterdam, 1976; Vols. I−III.
(5) (a) Lehn, J.-M.; Mascal, M.; DeCian, A.; Fischer, J. *J. Chem. Soc., Perkin Trans. 2* **1992**, 461. (b) Subramanian, S.; Zaworotko, M. *Can. J. Chem.* **1992**, *71*, 433. (c) Seto, C. T.; Whitesides, G. M. *J. Am. Chem. Soc.* **1991**, *113*, 9025. (d) Weber, E.; Finge, S.; Csoregh, I. *J. Org. Chem.* **1991**, *56*, 7881.

S0897-4756(96)00123-8 CCC: $12.00

Table 1. Physical Measurements of Anilinium L-Monohydrogen Tartrate and Anilinium D-Dibenzoyl Monohydrogen Tartrate Salts and Measured Powder SHG Intensities

entry	acid (mp/°C)	base (mp/°C)	salt (mp/°C)	SHG activity (salt vs urea) and code
1	L-tartaric acid (168−170)			0.91
2	D-dibenzoyl tartaric acid (89−91)			1.00
3	L-tartaric acid	2,6-dimethyl (12)	147	0.82 [**1**]
4	D-DBT	2,6-dimethyl (13)	171	0.86 [**2**]
5	D-DBT	2,3-dimethyl (2.5)	166−170[a]	0.79 [**3**]
6	D-DBT	2-methyl (−28)	165	*d* [**4**]
7	D-DBT	3-methyl[b] (−50)	144	0.91 [**5**]
8	D-DBT	3-methyl[c] (−50)	145−150[a]	0.88 [**6**]

[a] Decomposes during melting. [b,c] Stoichiometric variations (1:1 and 1:2) of the salt. [d] No detectable SHG activity.

noncentrosymmetric crystals for second harmonic generation (SHG).[7−11]

In our ongoing program to synthesize compounds which provide guidelines for the design of potential SHG materials, we have prepared systems involving multidirectional hydrogen bonding so as to produce good-quality single crystals which is a major criterion for eventual utilization in commercially viable nonlinear optical (NLO) devices. L-Tartaric acid is a chiral, dihydroxy, dicarboxylic acid. The monovalent tartrate anion has a propensity to initiate a motif resulting in infinite chains with very short O−H···O interactions between dicarboxylate anions[15] giving pointers to the design of potential future NLO materials. Networks built on hydrogen tartrates with polarizable cations[7,8] have been demonstrated to form new nonlinear optical materials. In all these studies, the resulting binary salts generate a supramolecular network indicating that subtle structural changes in the molecular features of either of the partners might result in altered networks optimizing the possibilities of producing new materials with NLO properties. The use of D-(+)-dibenzoyltartaric acid (DBT) as one of the partners has demonstrated the formation of altered crystallographic frameworks for generating materials which show SHG intensities of 1.4−1.6 times that of urea. The rationale for a clear understanding of structure−property correlation in these materials however requires a systematic analysis in terms of stoichiometry, substitution dependent geometry of the cations on one hand and specific interactions resulting due to the formation of the anionic framework on the other.

In this paper we report the syntheses and single-crystal X-ray structures of six new binary salts. The first three are 2,6-xylidinium-L-monohydrogen tartrate (**1**), 2,6-xylidinium-D-dibenzoyl monohydrogen tartrate (**2**), and 2,3-xylidinium-D-dibenzoyl monohydrogen tartrate (**3**). An attempt has been made to systematize the structural features in terms of packing of the three related but differently substituted cations. In the same vein, we also report the structures of 2-toluidinium-D-dibenzoyl monohydrogen tartrate (**4**) and 3-toluidinium-D-dibenzoyl monohydrogen tartrate (1:1, **5**) and 3-toluidinium-D-dibenzoyl tartrate (1:2, **6**) to explore the influence of stoichiometric variation on the crystal packing. The cations 2,6-xylidinium and 2,3-xylidinium were chosen essentially to investigate the distortions that might have originated in the anionic network of DBT due to steric bulk and location of their hydrogen-bond acceptor sites. The structure of 2,6-xylidinium-L-monohydrogen tartrate was also determined to compare the variations that have resulted due to the absence of bulky aromatic groups in these networks.

Experimental Section

All the amines used were purified by distillation under reduced pressure. L-Tartaric acid and D-dibenzoyl tartaric acid were obtained from Sigma. The salts were prepared by dissolving equimolar amounts of the corresponding acid and the respective base in methanol−water mixture and allowing the solvent to evaporate slowly at room temperature. The crystals which formed were filtered off and recrystallized from methanol, filtered, and dried. Melting points were examined in open capillaries and are uncorrected (Table 1). The formation of the salts was also characterized using powder X-ray studies using the STOE STADI/P powder X-ray diffractometer. The simultaneous TG/DTA curves were recorded on Polymer Labs Thermal Analysis Unit (STA-1500). The samples were heated at a heating rate of 15 °C/min under ambient conditions.

(6) (a) Chang, Y.-L.; West, M.-A.; Fowler, F. W.; Lauher, J. W. *J. Am. Chem. Soc.* **1993**, *115*, 5991. (b) Lauher, J. W.; Chang, Y.-L.; Fowler, F. W. *Mol. Cryst. Liq. Cryst.* **1992**, *211*, 99. (c) Simard, M.; Su, D.; Wuest, J. D. *J. Am. Chem. Soc.* **1991**, *113*, 4696. (d) Garcia-Tellado, F.; Gieb, S. J.; Goswami, S.; Hamilton, A. D. *J. Am. Chem. Soc.* **1991**, *113*, 9265. (e) Hollingsworth, M. D.; Santansiero, B. D.; Oumar-Mahamat, H.; Nichols, C. J. *Chem. Mater.* **1991**, *3*, 23. (f) Zhao, X.; Chang, Y.-L.; Fowler, F. W.; Lauher, J. W. *J. Am. Chem. Soc.* **1990**, *112*, 6627. (g) Etter, M. C.; Adsmond, D. A. *J. Chem. Soc., Chem. Commun.* **1990**, 589. (h) Etter, M. C.; Urbanczyk-Lipkowska, Z.; Zia-Ebrahimi, M.; Panunto, T. W. *J. Am. Chem. Soc.* **1990**, *112*, 8415.

(7) (a) Renuka, K.; Guru Row, T. N.; Prasad, B. R.; Subramanian, C. K.; Bhattacharya, S. *New J. Chem.* **1995**, *19*, 83. (b) Aakeroy, C. B.; Nieuwenhuyzen, M. *J. Am. Chem. Soc.* **1994**, *116*, 10983. (c) Watanabe, O.; Noritake, T.; Hirose, Y.; Okada, A.; Kuraucchi, T. *J. Mater. Chem.* **1993**, *3*, 1053. (d) Zyss, J.; Pecaut, J.; Levy, J. P.; Masse, R. *Acta Crystallogr.* **1993**, *B49*, 334. (e) Frankenbach, G. M.; Etter, M. C. *Chem. Mater.* **1992**, *4*, 272.

(8) (a) Bhattacharya, S.; Dastidar, P.; Guru Row, T. N. *Chem. Mater.* **1994**, *6*, 531. (b) Dastidar, P.; Guru Row, T. N.; Prasad, B. R.; Subramanian, C. K.; Bhattacharya, S. *J. Chem. Soc., Perkin Trans. 2* **1993**, 2419. (c) Aakeroy, C. B.; Hitchcock, P. B. *J. Mater. Chem.* **1993**, *3*, 1129. (d) Aakeroy, C. B.; Bahra, G. S.; Hitchcock, P. B.; Patell, Y.; Seddon, K. R. *J. Chem. Soc., Chem. Commun.* **1993**, 152. (e) Zyss, J.; Masse, R.; Bagieu-Beucher, M.; Levy, J.-P. *Adv. Mater.* **1993**, *5*, No. 2, 120. (f) Aakeroy, C. B.; Hitchcock, P. B.; Seddon, K. R. *J. Chem. Soc., Chem. Commun.* **1992**, 553. (g) Zyss, J. *Nonlinear Opt.* **1991**, *1*, 3. (h) Zyss, J.; Nicoud, J. F.; Coquillay, M. *J. Chem. Phys.* **1984**, *81*, 4160. (i) Zyss, J.; Berthier, G. *J. Chem. Phys.* **1982**, *77*, 3635.

(9) (a) Etter, M. C.; Huang, K. S. *Chem. Mater.* **1992**, *4*, 824. (b) Panunto, T. W.; Urbanczyk-Lipkowska, Z.; Johnson, R.; Etter, M. C. *J. Am. Chem. Soc.* **1987**, *109*, 7786.

(10) Etter, M. C.; Urbanczyk-Lipkowska, Z.; Zia-Ebrahimi, M.; Punnuto, T. W. *J. Am. Chem. Soc.* **1990**, *112*, 8415.

(11) (a) Masse, R.; Bagieu-Beucher, M.; Pecaut, J.; Levy, J.-P.; Zyss, *J. Nonlinear Opt.* **1993**, *V5*, 413. (b) Kotler, Z.; Hierle, R.; Josse, D.; Zyss, J.; Masse, R. *J. Opt. Soc. Am.* **1992**, *B9*, 534. (c) Bagieu-Beucher, M.; Masse, R.; Tranqui, D. *Z. Anorg. Allg. Chem.* **1991**, *606*, 59. (d) Masse, R.; Zyss, J. *Mol. Eng.* 1991, 1, 141. (e) Masse, R.; Durif, A. *Z. Kristallogr.* **1990**, *190*, 19. (f) Aakeroy, C. B.; Hitchcock, P. B.; Moyle, B. S.; Seddon, K. R. *J. Chem. Soc., Chem. Commun.* **1989**, 1856.

(12) Pecaut, J.; Le Fur, Y.; Masse, R. *Acta Crystallogr.* **1993**, *B49*, 535.

(13) (a) Reutzel, S. M.; Etter, M. C. *J. Phys. Org. Chem.* **1992**, *5*, 44. (b) Etter, M. C.; Reutzel, S. M. *J. Am. Chem. Soc.* **1991**, *113*, 2586.

(14) Russel, V. A.; Etter, M. C.; Ward, M. D. *J. Am. Chem. Soc.* **1994**, *116*, 1941.

(15) Leiserowitz, L. *Acta Crystallogr.* **1976**, *B32*, 775.

Table 2. Crystal and Refinement Data for 1−3

details	1	2	3
empirical formula	$C_{12}H_{17}O_6N{\cdot}0.5H_2O$	$C_{26}H_{25}O_8N$	$C_{26}H_{25}O_8N{\cdot}0.5H_2O$
formula wt	280	479	488
cryst size, mm	0.15 × 0.15 × 0.57	0.10 × 0.15 × 0.37	0.08 × 0.15 × 0.30
cryst syst	orthorhombic	monoclinic	monoclinic
space group	$P22_12_1$	$P2_1$	$P2_1$
unit cell dimensions			
a, Å	7.283(2)	7.906(1)	7.837(1)
b, Å	17.030(2)	24.757(1)	24.448(1)
c, Å	22.196(2)	13.166(1)	13.763(1)
β, deg		105.01(1)	105.69(1)
rflns to determine unit cell	25	24	25
F(000)	1184	1008	1028
V, Å^3	2753	2489	2538
Z	8	4	4
D_{calc}, g/cm^{-3}	1.366	1.280	1.284
radiation used	Mo Kα	Cu Kα	Cu Kα
linear abs coeff, cm^{-1}	1.069	7.577	7.696
temp, K	293	213	293
	Data Collection		
diffractometer	Enraf-Nonius CAD4	Rigaku AFC6R	Enraf-Nonius CAD4
scan method	$\omega/2\theta$		$\omega/2\theta$
rflns coll	2371	3991	4194
unique rflns	2157	3743	3500
2θ range, deg	$0 \le \theta \le 23.5$	$0 \le \theta \le 60.00$	$0 \le \theta \le 60.0$
h,*k*,*l* range	0−8,0−19,0−24	0−8,0−27,±14	0−8,0−27,±15
	Refinement		
refinement method	full-matrix LS on *F*	full-matrix LS on *F*2	full-matrix LS on *F*
parameters	496	632	641
goodness of fit	1.430	1.708	1.200
final *R* indexes	0.054	0.039	0.061
R and R_w for [$I > 3\sigma I$]	0.057	0.042	0.074
largest diff, hole and peak, e/Å^{-3}	−0.295, 0.314	−0.288, 0.251	−0.289, 0.241

The SHG intensities of the salts were measured using the standard powder technique[16] on a polycrystalline sample ground to uniform grain size (Table 1). The 1.06 μm line of a pulsed Q-switched Nd:YAG laser (Quanta Ray, DCR-2A) with a pulse duration of 8 ns was used to generate second harmonic signals from the samples. The forward scattered SHG signals were collected using collection optics and passed through a filter which transmits only 532 nm radiation. The intensities of the incident laser beam and the SHG radiation were measured using an energy ratio meter (LPC RJ-7620) equipped with pyroelectric (LPC RJP-735) and silicon (LPC RJP-765) detectors. The measured SHG intensities of the samples were normalized with respect to that of urea. The powder samples used for these SHG measurements were characterized for particle size on a JEOL JEM 200 CX electron microscope operated at 200 kV. The samples were prepared by ultrasonic dispersion of the powders in hexane medium, and the resultant slurry was deposited on a holey carbon grid (200−400 mesh). Bright-field images were recorded at different magnifications and the particle size distribution was found to be in the range 2−16 μm.

The crystals of **5** and **6** appeared well formed but had mosaicity distributions over large ranges (0.8−2.5) and diffracted poorly. We could harness a reasonable data set with difficulty. It appeared as if the crystals are twinned with the twinning possibly developing along the longest *C* axis. It was not possible to uniquely identify reflections corresponding to one of the twins. The starting reflections used for indexing were taken from a group of reflections which had mosaicities less than or equal to 1. Also, care was taken to see that reflections with larger values of *L* were included in the indexing procedure. The implications of such restrictions are discussed later on. The stabilities and orientations in all the cases were monitored by measuring three standard reflections (see Tables 2 and 3) every 3600 s of exposure time; the orientation was checked every 400 reflections and no significant fluctuations in their intensities was observed. The data were corrected for Lorentz and polarization effects but not for extinction and absorption effects.

The structures were solved by direct methods using SHELXS 86[17] and all the non-hydrogen atoms of **1**−**4** were refined anisotropically by the full-matrix least-squares program SHELX 76.[18] Structures **5** and **6** were refined using the programme SHELXL 93.[19] The hydrogen atoms of **1**, **2**, and **4** were located on a difference map, and their positional and thermal parameters were allowed to refine freely for a few cycles of refinement. All the hydrogen atoms of **3** except HO5 were fixed geometrically at calculated positions and were not refined. None of the hydrogen parameters in all these structures were refined during the final cycles of refinement, but their contributions to the structure factor calculations were considered. The hydrogen atoms attached to the amine nitrogen atoms and to the phenyl rings of **5** and **6** were fixed geometrically and were not refined further though their contributions to the structure factor calculations were considered. Details of the data collection, reduction, and refinement are summarized in Tables 2 and 3. The anionic network patterns and packing of the cations between them[22] and the hydrogen-bonding patterns[23] are shown in Figures 1a,b, 2a,b, 3a,b, 4a,b, 5a,b, and 6a,b, respectively. The hydrogen-bonding angles and distances are tabulated in Tables 4−9.

Results

Structure of 1. A general feature of the crystal structures of tartaric acid salts is the presence of

(16) Kurtz, S. K.; Perry, T. T. *J. Appl. Phys.* **1968**, *39*, 3798.

(17) Sheldrick, G. M. SHELXS86, program for the solution of crystal structures, University of Gottingen, Germany, 1986.

(18) Sheldrick, G. M. SHELX76, program for crystal structure determinations, University of Cambridge, England, 1976.

(19) Sheldrick, G. M. SHELXL 93, program for crystal structure refinement, University of Cambridge, England, 1993.

(20) Parafonry, A.; Tinant, B.; Declercq, J. P.; Van Meerssche, M. *Bull. Soc. Chim. Belg.* **1983**, *92*, 437.

(21) (a) Etter, M. C. *Acc. Chem. Res.* **1990**, *23*, 120. (b) Etter, M. C.; MacDonald, J. C. *Acta Crystallogr.* **1990**, *B49*, 256.

(22) Insight II, a program for molecular modeling, BIOSYM, USA.

(23) Motherwell, W. D.; Clegg, W. PLUTO, Program for plotting molecular and crystal structures, University of Cambridge, England, 1977.

Table 3. Crystal and Refinement Data for 4−6

details	4	5	6
empirical formula	$C_{25}H_{23}O_8N$	$C_{25}H_{23}O_8N$	$C_{32}H_{36}O_{10}N$
formula wt	465	465	608
cryst size, mm	0.34 × 0.20 × 0.25	0.08 × 0.25 × 0.90	0.45 × 0.35 × 0.13
cryst syst	orthorhombic	triclinic	triclinic
space group	$P2_12_12_1$	$P1$	$P1$
unit cell dimensions			
a, Å	13.553(2)	7.916(3)	7.828(3)
b, Å	15.869(3)	11.467(6)	8.233(1)
c, Å	22.123(2)	14.203(8)	24.888(8)
α, deg	90.0	96.44(4)	93.98(2)
β, deg	90.00	98.20(5)	94.58(3)
γ, deg	90.00	110.55(5)	89.99(2)
rflns to determine unit cell	25	22	25
F(000)	1952	1176	1595
V, Å^3	8	2	2
Z	8	2	2
D_{calc}, g/cm^{-3}	1.300	1.314	1.267
radiation used	Mo Kα	Mo Kα	Mo Kα
linear abs coeff, cm^{-1}	0.913	0.990	0.950
temp, K	293	158	293
	Data Collection		
diffractometer	Enraf-Nonius CAD4	Siemens P4	Enraf-Nonius CAD4
scan method	$\omega/2\theta$	ω	$\omega/2\theta$
rflns coll	3928	3519	5047
unique rflns	3665	3519	5003
2θ range, deg	$0 \le \theta \le 23.5$	$5 \le \theta \le 50.0$	$0 \le \theta \le 23$
h,k,l range	0−15,0−17,0−24	0−8,±12,±16	0−8,±9,±27
	Refinement		
refinement method	full-matrix LS on F	full-matrix LS on $F2$	full-matrix LS on F^2
parameters	614	619	787
goodness of fit	0.994	0.862	1.113
final R indexes	0.042	0.069	0.153
R and R_w	0.050 [$I > 3\sigma(I)$]	0.168 [$I > 2\sigma(I)$]	0.338 [$I > 2\sigma(I)$]
largest diff, hole and peak, e/Å^{-3}	−0.168, 0.239	−0.332, 0.474	−0.538, 1.168

extensive hydrogen bonding. Tartaric acid and its derivatives show a feature wherein the hydroxyl groups present in the acid are gauche to each other.[20] These features are preserved in **1**. The structure of **1** has two molecules in the asymmetric unit ($Z = 8$) and the two monohydrogen tartrate anions are dispersed in nearly identical conformations, their backbone torsion angles involving the atoms C(1)−C(2)−C(3)−C(4) and C(1′)−C(2′)−C(3′)−C(4′) being 171.6(0.4)° and 171.0(0.4)° and the dihedral angles (about the hydroxyl groups) of the atoms O(3)−C(2)−C(3)−O(4) and O(3′)−C(2′)−C(3′)−O(4′) being −70.0(0.5)° and −70.6(0.5)°, respectively. This shows that the two hydroxyl groups are also gauche with respect to each other. The amines are protonated via the exocyclic nitrogen atoms N(1) and N(2). This is clearly seen by considering the distance between C(19) and N(1) and C(19′) and N(2).[8b]

The hydrogen-bonding pattern of **1** can be described as follows. There are infinite chains of anions held together by hydrogen bonds of the type $COO^-\cdots HO_2C$ involving the short O−H···O (∼2.5 Å) contacts between the anions in a "head-to-tail" (CO_2H-COO^-) fashion (Figure 1a). The 2,6-xylidinium cations, arranged antipolar to each other, cross-link such chains using hydrogen bonds to give rise to a network (Figure 1b, Table 4). A solvent water molecule of crystallization holds adjacent, parallel, infinite chains of the anions together. The water molecule acts as a bridge by accepting the hydrogen atom from the hydroxyl group of the anion [O(7)···O(4) = 2.679 Å] and by hydrogen bonding to the carboxylate end of the anions [O(1′)···O(7) = 2.814 Å and O(5)···O(7) = 2.771 Å]. The infinite chains form a homogeneous hydrogen-bonded network, and there is no cross patterning among the two independent molecules in the asymmetric unit or the ones generated by translational symmetry. To understand the hydrogen-bonding pattern, we have resorted to the graph set analysis developed by Etter which is a systematic and simple method to identify and classify hydrogen-bonded motifs in a wide variety of compounds.[21] The first-order network in **1** is therefore assigned to be of the type $N_1 = 9D2C_1^1$ (7), which means that there are nine simple, dimeric motifs and two infinite chains of repeat unit seven running throughout the crystal lattice.

Structure of 2. The anion used in **2** is D-dibenzoyl tartrate instead of L-hydrogen tartrate. The crystal structures of diacyl tartaric acids also show a conformation in which the −COOH groups are anti and the O-acyl groups are gauche to each other.[20] This feature is seen in **2** (and also in **3**). Since $Z = 4$, the two independent dibenzoyl monohydrogen tartrate anions are in different conformations. The backbone torsion angles and the ones involving the hydroxyl groups are as follows: C(1)−C(2)−C(3)−C(4) = 175.5(0.9)°, C(1′)−C(2′)−C(3′)−C(4′) = −174.3(1.0)° and O(3)−C(2)−C(3)−O(4) = −59.7(0.9)°, O(3′)−C(2′)−C(3′)−O(4′) = −58.1(1.1)° and as in **1** the hydroxyl groups are gauche to each other.

However the arrangement of the cations is unlike that in **1**. They are not arranged antipolar to each other as in **1** and hence they contribute to the overall dipole moment of the molecule (Figure 2a). The absence of solvent of crystallization, e.g., water in this structure is noteworthy and the anions form infinite chains through short O−H···O type of hydrogen bonds (Figure 2b, Table 5). The amines hold two such parallel chains

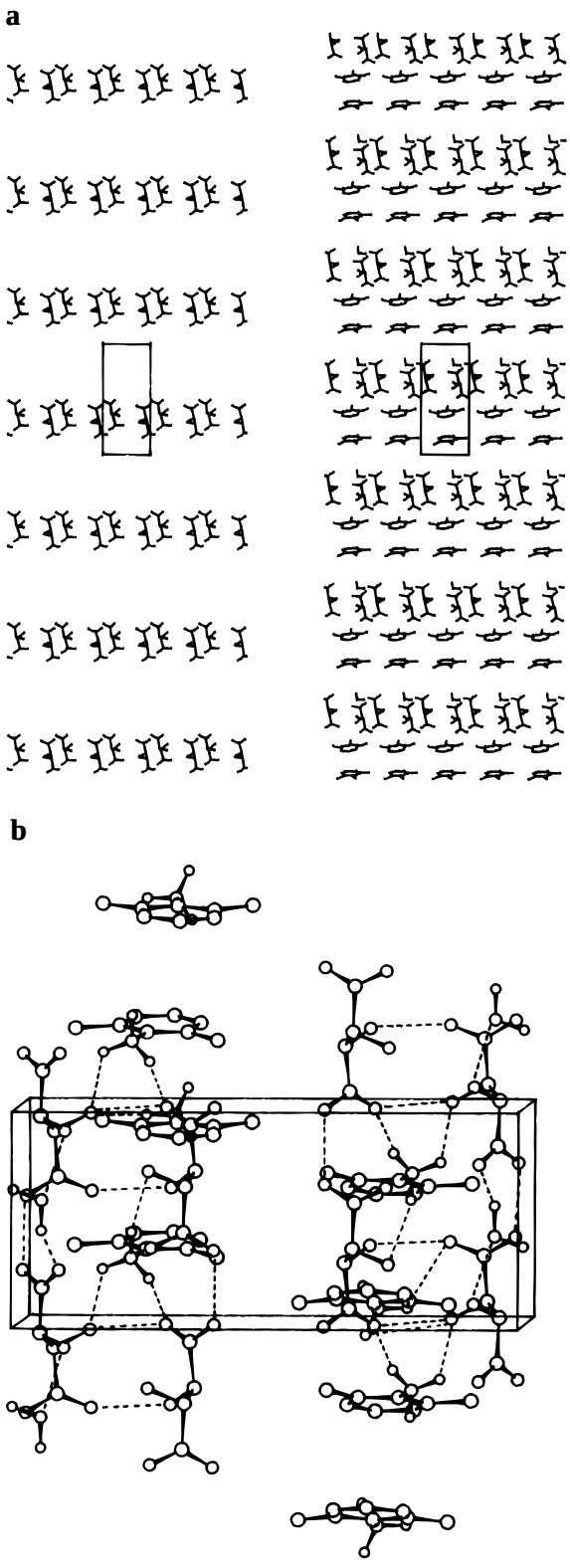

Figure 1. (a) Anionic network and molecular packing in compound **1**. (b) Hydrogen-bonding pattern of compound **1**.

together by hydrogen bonds through the amine nitrogen atoms (Table 5). The first-order network of **2** has been assigned to be of the type $N_1 = 5D2C_1^1(7)$. Thus there are five simple, dimeric motifs and two infinite chains of repeat unit seven.

Structure of 3. The cation in **3** differs from the cation in **2** by a change in the position of one of the methyl groups in the amine. **3** also crystallizes in the same space group as **2** ($P2_1$, $Z = 4$) but along with a

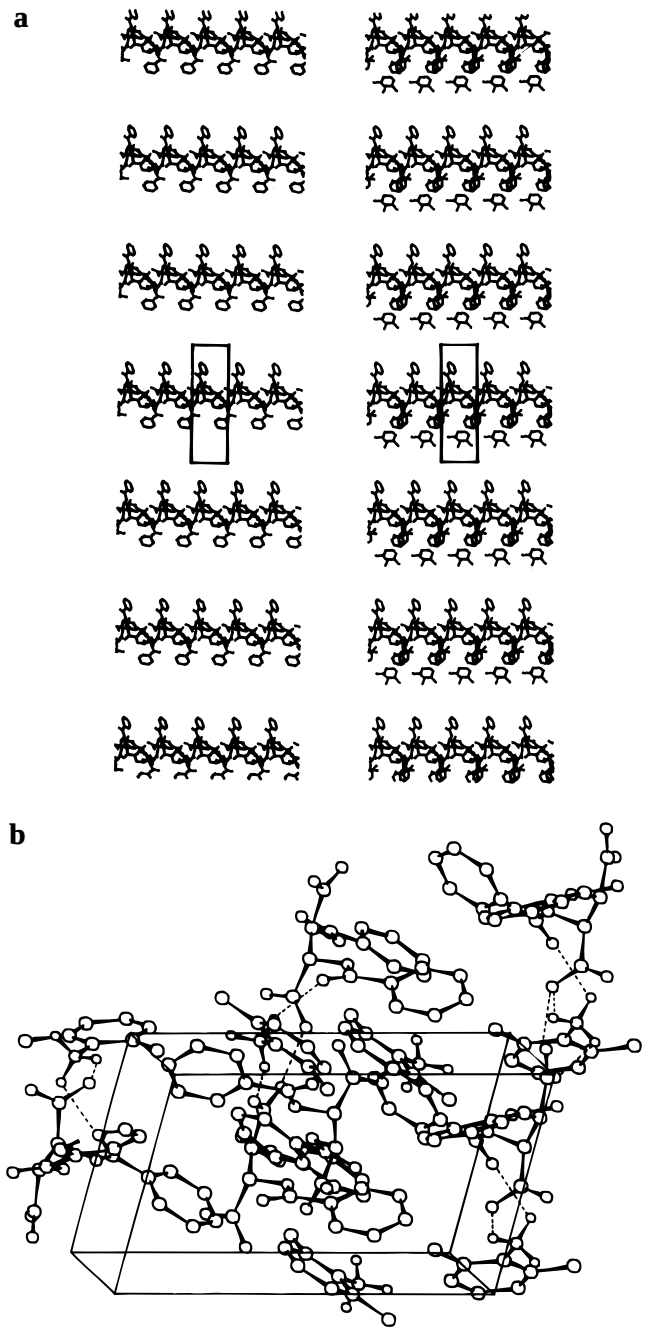

Figure 2. (a) Anionic network and molecular packing in compound **2**. (b) Hydrogen-bonding pattern of compound **2**.

water molecule of crystallization which makes the packing density higher than that of **2**. Interestingly, **2** and **3** have nearly the same unit-cell parameters. The two anionic units have different conformations and the backbone torsion angles are C(1)−C(2)−C(3)−C(4) = 178.5(0.8)°, C(1′)−C(2′)−C(3′)−C(4′) = 174.8(0.9)° and those concerning the hydroxyl groups are O(3)−C(2)−C(3)−O(4) = 64.5(0.8)° and O(3′)−C(2′)−C(3′)−O(4′) = 54.2(0.9)°, respectively. However, the hydrogen-bonding pattern here is similar to **2**, the anions forming two separate, parallel, infinite chains (Figure 3b, Table 6) interlinked by N−H···O hydrogen bonds provided by the nitrogen atoms of the cations. The water molecule stabilizes the structure by providing additional hydrogen bonds between the cations and the anions. The SHG activity also does not show any significant variation from that of **2** (Table 1). The first-order network of **3** can be described as $N_1 = 6D2C_1^1(7)$; thus there are

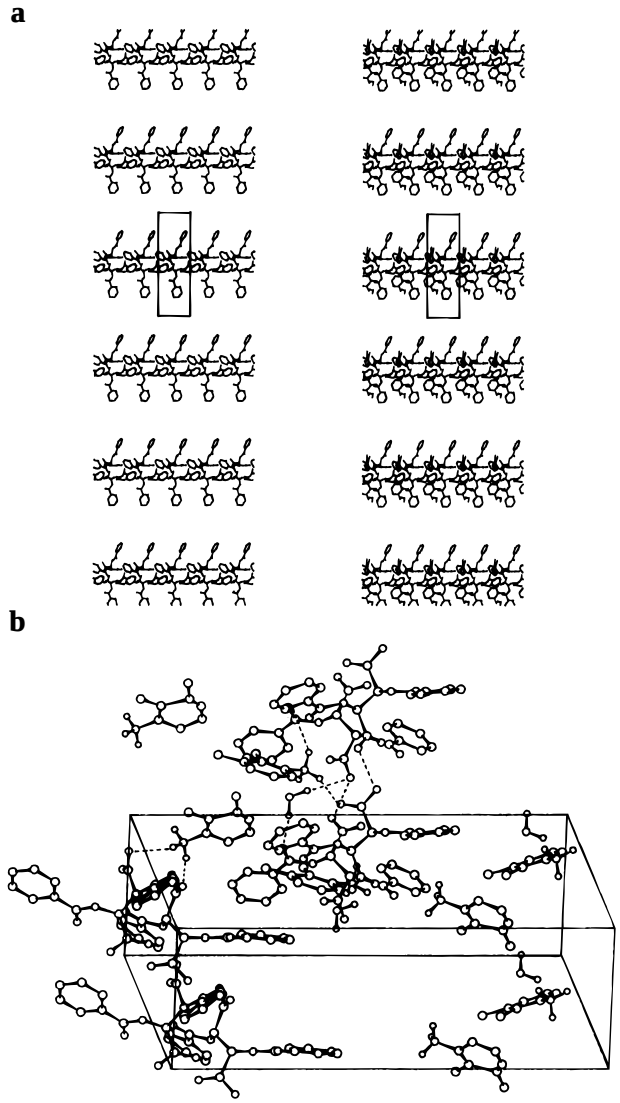

Figure 3. (a) Anionic network and molecular packing in compound **3**. (b) Hydrogen-bonding pattern of compound **3**.

six simple, dimeric motifs and two infinite chains of repeat unit seven. We see that though the number of simple, dimeric motifs vary in these three structures, the number of infinite chains is constant.

Structure of 4. **4** was studied to analyze the effect of substituent variation on the amine over the crystal packing (Figure 4a). The conformation of the two anions in the asymmetric unit ($Z = 8$) are distinctly different from each other. The torsion angles concerning the backbone and the hydroxyl groups being C(1)−C(2)−C(3)−C(4) = 164.9(0.3)°, C(1′)−C(2′)−C(3′)−C(4′) = 171.4(0.2)°, O(3)−C(2)−C(3)−O(4) = 59.0(0.3)°, and O(3′)−C(2′)−C(3′)−O(4′) = 48.1(0.3)°, respectively. The hydrogen-bonding pattern here involves both the dibenzoyl monohydrogen tartrate anions in the asymmetric unit and they hydrogen bond to each other in a "head to tail" arrangement forming a single infinite chain of the type $CO_2^-\cdots H'O_2C'$ and $CO_2'^-\cdots HO_2C$ even though each one has to be designated as independent chains for Etter's analysis. This feature is hitherto unobserved in this family of salts of tartaric acid and its derivatives with aromatic amines studied by us so far (Table 7). The first-order network is assigned as $N_1 = 6D2C_1^1(7)$. **4** has six simple, dimeric motifs and two infinite chains with repeat unit seven.

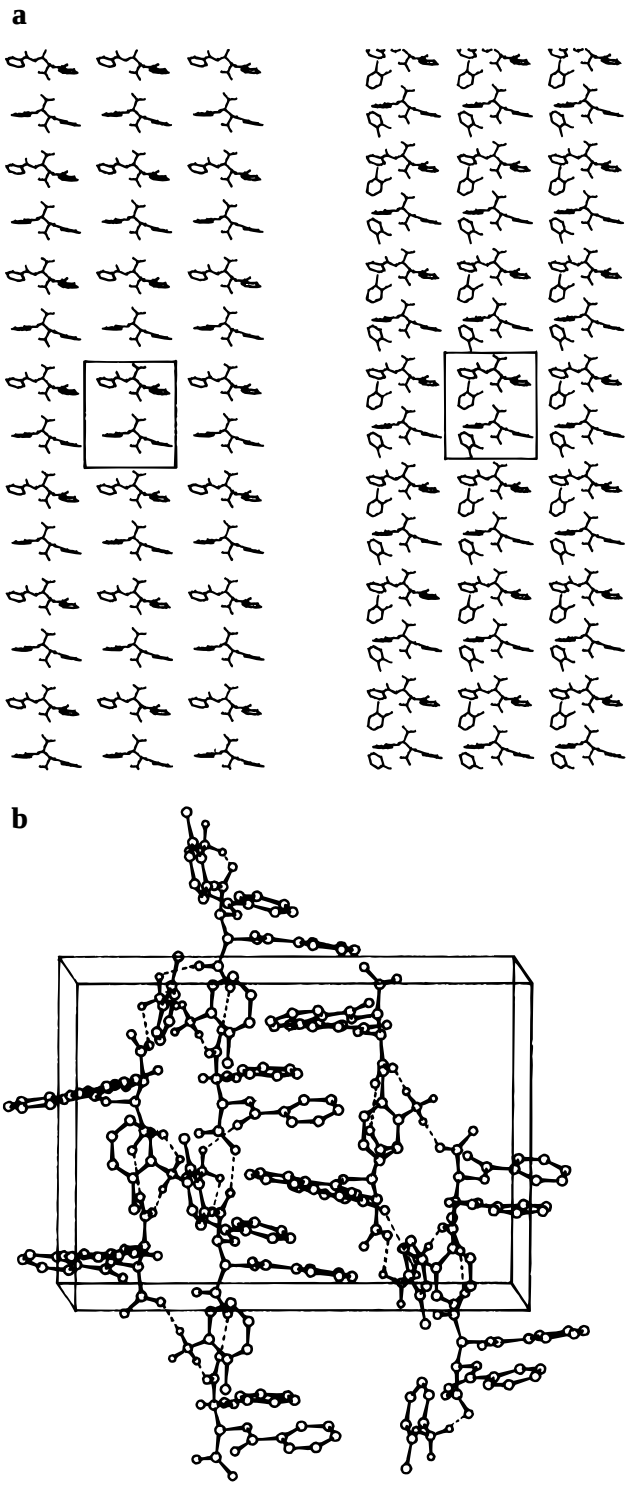

Figure 4. (a) Anionic network and molecular packing in compound **4**. (b) Hydrogen-bonding pattern of compound **4**.

Structure of 5. **5** differs from **4** in that there is a variation in the position of the substituent in the cation (Figure 5a). The conformation of the two anions in the asymmetric unit ($Z = 2$) are nearly similar to each other. The backbone torsion angles are C(1)−C(2)−C(3)−C(4) = −173.7(0.1)°, C(1′)−C(2′)−C(3′)−C(4′) = −174.8(0.1)°, and the torsion angles with respect to the hydroxyl groups are O(3)−C(2)−C(3)−O(4) = −61.6(0.1)°, O(3′)−C(2′)−C(3′)−O(4′) = −62.5(0.2)°, respectively. **5** has two infinite, parallel chains of anions held together by the N−H···O interactions provided by the cations as in the previous cases (Figure 5b, Table 8) without cross-

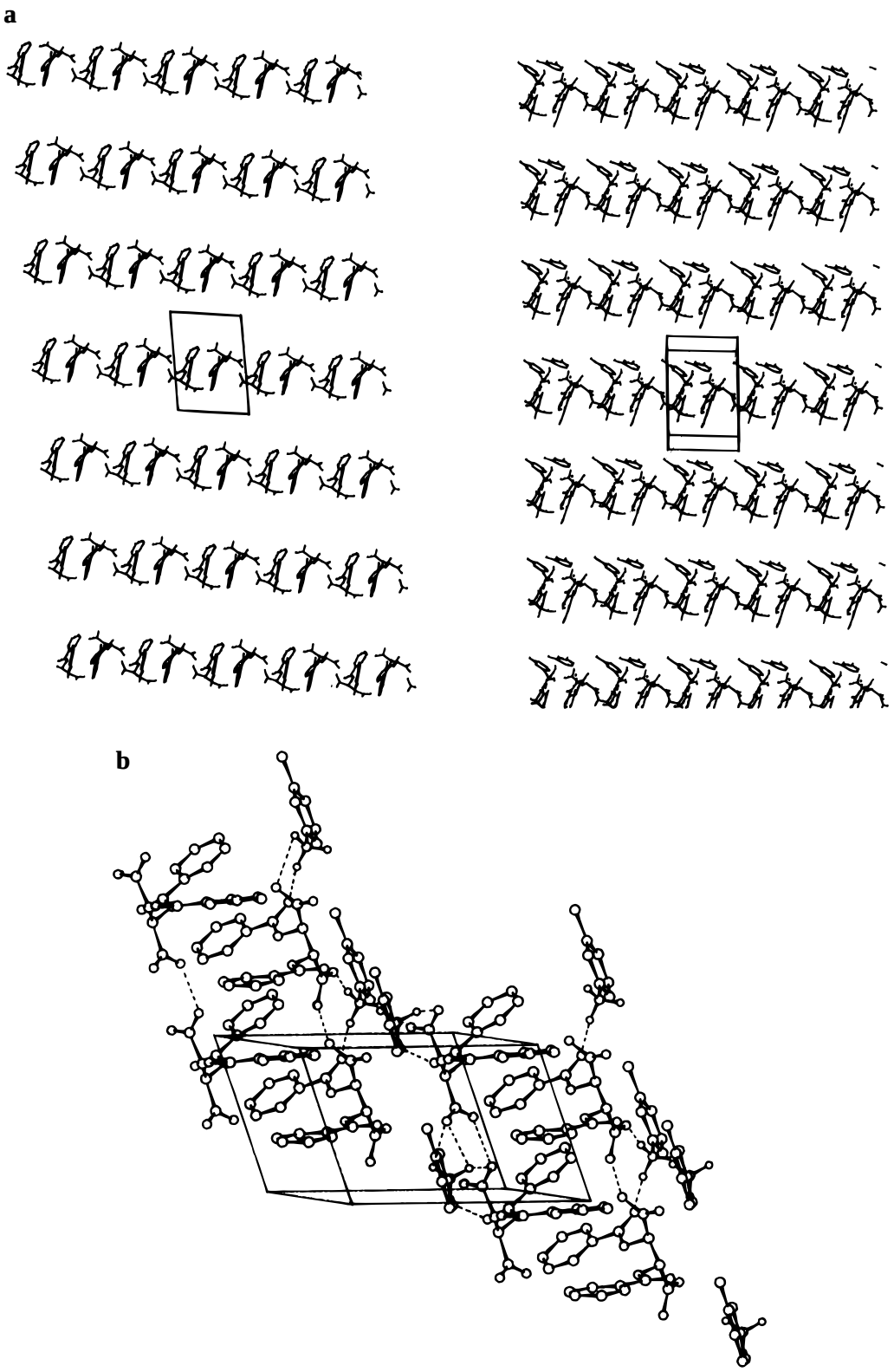

Figure 5. (a) Anionic network and molecular packing in compound **5**. (b) Hydrogen-bonding pattern of compound **5**.

patterning among the chains. The SHG activity of this salt is equivalent to urea. The first-order network is $N_1 = 5DD_1^2\ 2C_1^1$ (7) (ie) **5** has five simple, dimeric motifs, one bifurcated hydrogen bond and two infinite chains of repeat unit seven.

Structure of 6. Structure **6** is a stoichiometric variation of **5** where the ratio of the amine to the acid is 2:1. This structure differs vastly from **5** in its packing features (Figure 6a) and in its hydrogen-bonding pattern. In this structure $Z = 2$ and there are four water molecules of crystallization in the unit cell. The conformations of the DBT moieties are not very different and the torsion angles concerning the backbone and the hydroxyl groups being C(1)−C(2)−C(3)−C(4) = 174.7(0.1)°, C(1′)−C(2′)−C(3′)−C(4′) = 173.6(0.8)°, O(3)−C(2)−C(3)−O(4) = −73.5(0.1)°, and O(3′)−C(2′)−C(3′)−O(4′) = −70.7(0.4)°, respectively. The hydrogen-bonding pattern in this structure is totally different from the other structures described above. The infinite chain of hydrogen-bonded anionic network found in the previous

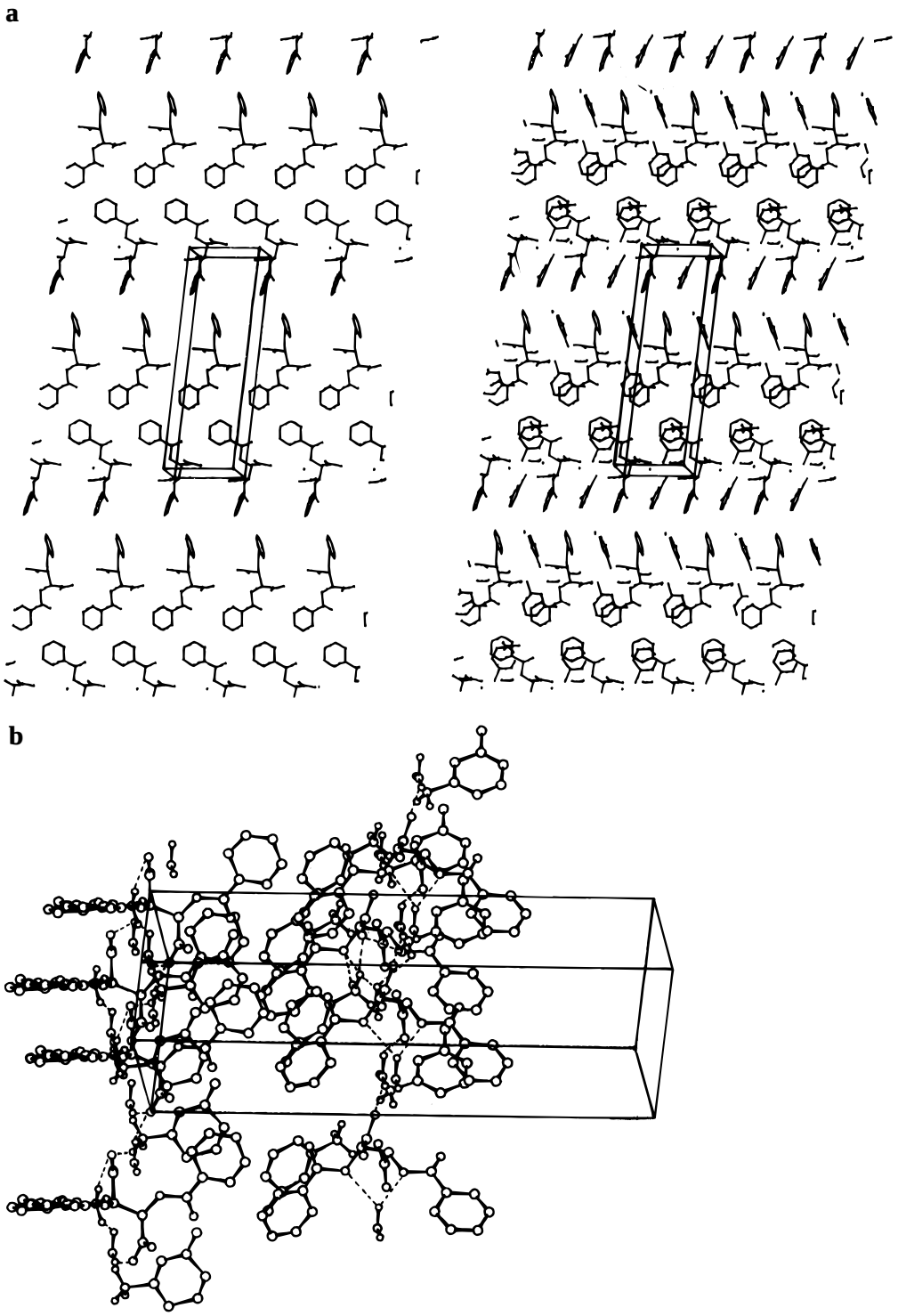

Figure 6. (a) Anionic network and molecular packing in compound **6**. (b) Hydrogen-bonding pattern of compound **5**.

structures is absent here, and the overall stability of the molecule is provided mainly by hydrogen bonding involving the water molecules of crystallization (Figure 6b, Table 9). The SHG activity of **6** is 0.5 times that of urea and the first-order network is given as $N_1 = 20D$, or **6** has 20 simple, dimeric motifs.

Discussion

The study of the above-mentioned six structures in terms of their hydrogen-bonding potential provides useful pointers to the design of networks directed toward SHG-active materials. Even though these salts do not show SHG signals greater than that of urea, this analysis brings out the essential features in these motifs. Owing to the presence of two benzoyl groups, the network generated by the DBT anions provide variability in the framework. An additional orientational restraint due to the presence of the phenyl rings in DBT is seen especially since the cations are aromatic. The network results from one-dimensional chains running parallel to each other and it is interesting to note that the interlayer hydrogen bonds are *longer* compared to the chain hydrogen bonds. This suggests that the incorporation of the cations between the infinite chains is a general feature while their orientation

Table 4. Geometry of the Hydrogen Bonds in 1

D−H···A[a]	*r*(H···A)/Å	*r*(D···A)/Å	(D−H···A)/deg
O(4′)−H(O4′)···O(1)	1.669	2.712	156.69
N(1)−H(1A)···O(3)	1.921	2.804	153.56
O(3)−H(O3)···O(6′)	1.920	2.828	137.18
O(4)−H(O4)···O(7)	1.694	2.679	155.80
O(5′)[1]−H(O5′)···O(1′)	1.654	2.501	177.31
N(1)−H(1C)···O(1)[2]	1.829	2.730	157.94
O(6)[1]−H(O6)···O(2)	1.585	2.510	170.77
O(7)−H(O7A)···O(1′)[3]	1.604	2.814	168.25
N(2)−H(2A)···O(4)[4]	1.932	2.792	133.63
N(2)−H(2B)···O(2′)	2.008	2.705	144.59
N(2)−H(2C)···O(3′)[6]	1.877	2.866	147.33

[a] Symmetry notations: [1](1 + *X*, *Y*, *Z*), [2](*X* − 1, *Y*, *Z*), [3](1 − *X*, 0.5 + *Y*, 0.5 − *Z*), [4](*X* − 1, 1.5 − *Y*, 0.5 + *Z*), [5](−*X*, 1.5 − *Y*, 0.5 + *Z*), [6](−*X* − 1, 1.5 − *Y*, 0.5 + *Z*).

Table 5. Geometry of the Hydrogen Bonds in 2

D−H···A[a]	*r*(H···A)/Å	*r*(D···A)/Å	(D−H···A)/deg
O(7)···H(1A)−N(1)	1.892	2.883	161.04
N(1)−H(1B)···O(5)[1]	1.705	2.717	167.42
O(1)···H(O1′)−O(5′)[1]	1.597	2.439	171.56
N(1)−H(1C)···O(6′)[1]	1.884	2.726	152.66
O(1)···H(O6)−O(6)[1]	1.597	2.459	132.01
O(2′)···H(2A)−N(2)[4]	1.835	2.722	158.90
O(2)[3]···H(2C)−N(2)[4]	1.735	2.749	161.29

[a] Symmetry notations: [1](*X* + 1, *Y*, *Z*), [2](*X*, *Y*, 1 + *Z*), [3](*X*, *Y*, *Z* − 1), [4](1 − *X*, 0.5 − *Y*, 1 − *Z*).

Table 6. Geometry of the Hydrogen Bonds in 3

D−H···A[a]	*r*(H···A)/Å	*r*(D···A)/Å	(D−H···A)/deg
N(1)−H(1A)···O(2′)[1]	1.885	2.806	139.42
N(1)−H(1C)···O(8)[1]	1.822	2.882	161.92
O(1)···HO(5)−O(5)[2]	1.397	2.454	155.70
O(6′)···O(1′)[2]	*b*	2.449	*b*
N(1)−H(1B)···O(2)[3]	1.710	2.760	171.70
N(2)−H(2B)···O(5′)[4]	1.959	2.754	128.98
O(9)−HO(9B)···O(7)[4]	1.797	2.852	154.30
O(9)−HO(9A)···O(1)[4]	2.033	2.938	139.33

[a] Symmetry notations: [1](*X*, *Y*, 1 + *Z*), [2](*X* + 1, *Y*, *Z*), [3](*X* − 1, *Y*, 1 + *Z*), [4](1 − *X*, *Y* + 0.5, −*Z*), [5](−*X*, *Y* + 0.5, −*Z*). [b] Hydrogen atom not located.

Table 7. Geometry of the Hydrogen Bonds in 4

D−H···A[a]	*r*(H···A)/Å	*r*(D···A)/Å	(D−H···A)/deg
O(1′)−H(O1′)···O(6)	1.306	2.454	163.61
N(1)−H(1C)···O(5)	1.811	2.672	162.55
N(2)−H(2A)···O(5′)	1.767	2.789	168.49
N(2)−H(2C)···O(7)[1]	1.897	2.837	162.09
O(1)[1]−H(O1)···O(6′)	1.212	2.441	152.62
N(1)−H(1B)···O(2)[2]	1.774	2.767	165.37
N(2)−H(2B)···O(2′)[2]	1.729	2.715	159.47
N(1)−H(1A)···O(8′)[3]	1.942	2.896	157.25

[a] Symmetry notations: [1](*X*, 1 + *Y*, *Z*), [2](1 − *X*, 0.5 + *Y*, 0.5 − *Z*), [3](1 − *X*, 0.5 − *Y*, 0.5 − *Z*).

depends on the cross-linkages of hydrogen bonds between the layers.

Role of Solvent. The packing modes and the hydrogen-bond characteristics are recast in the presence of solvent molecules incorporated into the crystal structure. These features are clearly seen in **3** and **6**. In **3**, there is a water molecule of crystallization that appears to widen the space between the infinite chains (Figure 3b) by providing additional interchain hydrogen bonds. The structure of **6** in this context is significant since as many as four water molecules of crystallization are accommodated within the lattice to cause gross disruption of the infinite chain pattern. To investigate further the features of such destabilizing solvent-mediated interactions, we have carried out a careful thermogravimetric analysis of **3** and **6**. The hydrogen-bond network of **3** on removal of the solvent water molecule by heating crumbles, resulting in total decomposition of the material. However, structure **6** shows a remarkable behavior on heating. The DTA/TG plot indicates the presence of a stabilized phase after the initial transformation at ∼74 °C (Figure 7). We have characterized the high-temperature phase by powder X-ray diffraction studies. The powder XRD patterns at 85 °C (Figure 8i−k) are identical with that of compound **5** (Figure 8l) recorded at 25 °C. Figure 8k has been recorded to demonstrate that the resulting phase at 85 °C is indeed stable and resembles the diffraction pattern of compound **5** on cooling to 25 °C (Figure 8l). The diffractograms (Figure 8a−k) demonstrate clearly that structure **6** transforms on heating to structure **5**, by losing the solvent water molecules followed by one of the amines from the crystal lattice. The evolution of **5** from **6** proceeds gradually

Table 8. Geometry of the Hydrogen Bonds in 5

D−H···A[a]	*r*(H···A)/Å	*r*(D···A)/Å	(D−H···A)/deg
N(1)−H(1C)···O(8)	2.064	2.879	151.50
O(6)···H(2)−O(2)[1]	1.649	2.443	162.40
O(5′)−H(5′)···O(2′)[1]	1.648	2.459	143.50
N(1)−H(1A)···O(1)[1]	1.855	2.745	173.60
N(1)−H(1B)···O(6′)[2]	1.838	2.696	163.80
N(2)−H(2B)···O(1′)[2]	1.866	2.752	174.70
N(2)-H(2B)···O(5′)[3]	2.043	2.893	160.40
N(2)−H(2A)···O(8′)[3]	1.817	2.657	160.00

[a] Symmetry notations: [1](*X* + 1, *Y*, *Z*), [2](*X*, 1 + *Y*, *Z*), [3](*X* − 1, *Y*, *Z*), [4](*X* − 1, *Y* + 1, *Z*).

Table 9. Geometry of the Hydrogen Bonds in 6

D−H···A[a]	*r*(H···A)/Å	*r*(D···A)/Å	(D−H···A)/deg
O(5)···O(1S)	*c*	2.896	*c*
O(1)···O(2S)	*c*	2.768	*c*
O(5′)···O(3S)	*c*	2.907	*c*
O(1′)···O(4S)	*c*	2.781	*c*
N(1)−H(1A)···O(6)[b]	2.216	2.746	117.76
N(1)−H(1C)···O(2S)[b]	2.194	2.696	115.21
N(3)−H(3B)···O(4S)	1.802	2.676	166.84
N(3)−H(3C)···O(6′)	1.925	2.780	160.70
N(4)−H(4B)···O(6′)	1.860	2.721	162.05
N(1)−H(1B)···O(2)[1]	2.146	2.839	134.29
N(3)−H(3A)···O(2′)[1]	2.101	2.858	142.45
N(4)−H(4A)···O(3S)[1]	1.896	2.689	147.45
N(4)−H(4C)···O(2′)[1]	2.161	2.884	130.85
O(1S)···O(1)[2]	*c*	2.687	*c*
O(4S)···O(5′)[2]	*c*	2.716	*c*
O(2S)···O(5)[3]	*c*	2.735	*c*
O(3S)···O(1′)[3]	*c*	2.686	*c*
N(2)−H(2C)···O(6)[3]	2.111	2.681	121.06
N(2)−H(2A)···O(2)[4]	2.005	2.788	145.94
N(2)−H(2B)···O(1S)[4]	2.043	2.711	130.92

[a] Symmetry notations: [1](*X* − 1, *Y*, *Z*), [2](*X*, *Y* + 1, *Z*), [3](*X*, *Y* − 1, *Z*), [4](*X* − 1, *Y* − 1, *Z*). [b] Possible hydrogen bonds. [c] Hydrogen atom not located.

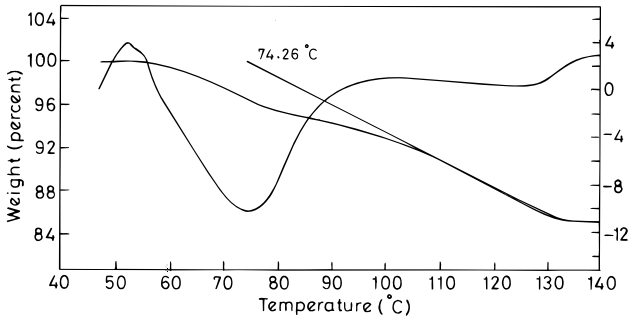

Figure 7. Thermogravimetric analysis of 6.

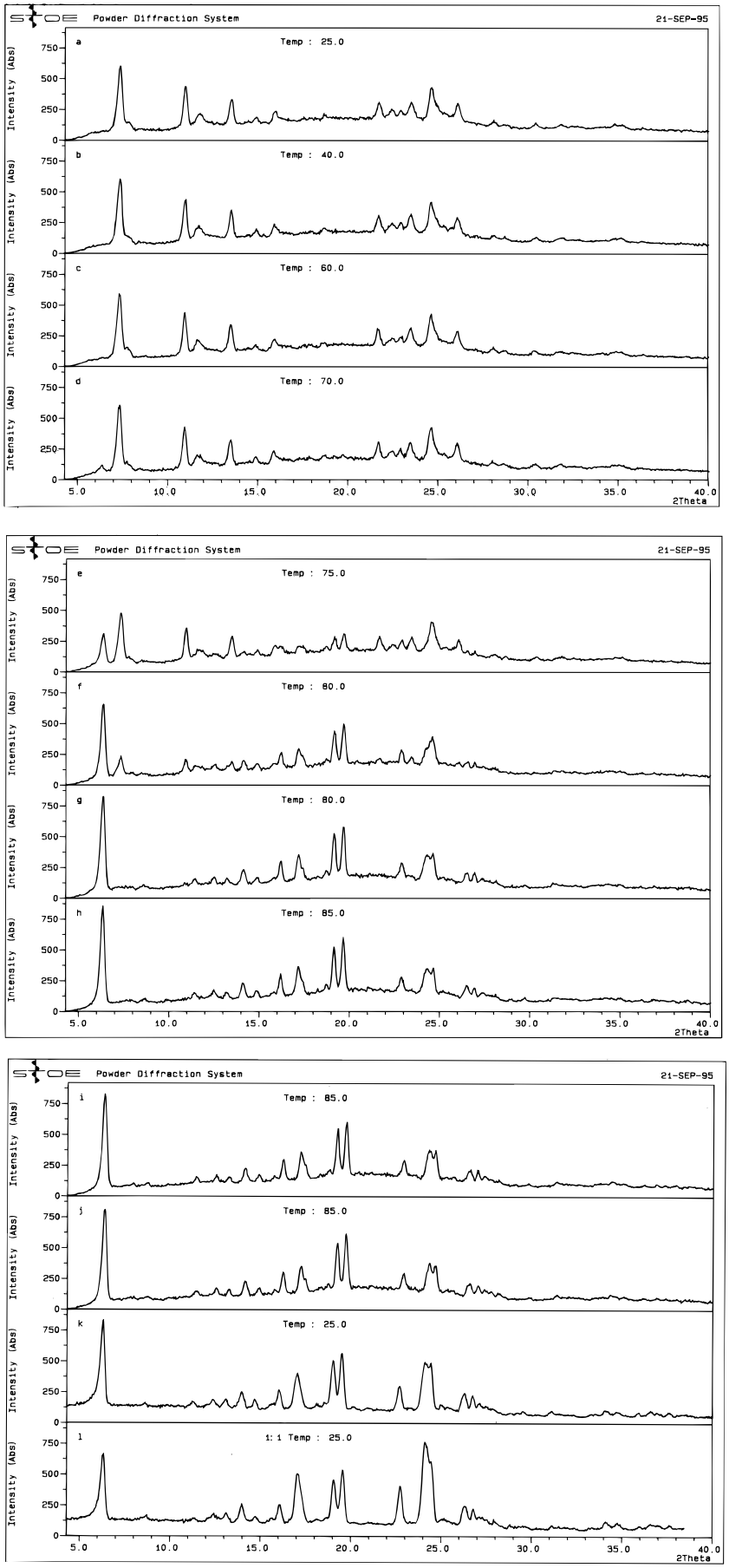

Figure 8. High-temperature powder X-ray diffraction pattern of **6** (a, 25 °C; b, 40 °C; c, 60 °C; d, 70 °C; e, 75 °C; f, 80 °C; g, 80 °C; h, 85 °C; i, 85 °C; j, 85 °C; k, 25 °C; l, compound **5** at 25 °C).

as can be seen from the diffractograms recorded in steps of 5 °C from 25 to 85 °C.

Conclusions

We have demonstrated that the design of materials with potential SHG properties emanate from self-assembled systems involving multidirectional hydrogen bonding. On the basis of the six structures discussed above, it appears that such solids with desired properties could be assembled using either fixed frameworks or by the judicious alteration of frameworks by substituents and/or by chemical variants. The crystal packing dictates the orientation of the components in the lattice, and the hydrogen-bond motifs provide predictability to augment the nonlinear response. The presence of solvent water generally deters the formation of the infinite hydrogen-bond framework but does not seem to have a direct bearing on the SHG activity. These results add to our understanding of the building of hydrogen-bond networks around specific anions or cations used in the engineering of crystalline NLO materials.

Acknowledgment. We gratefully acknowledge the financial support from STC, India. We thank CSIR, India, for funding (T.N.G.) and for a fellowship (R.K.). We also thank the Department of Chemistry, University of Canterbury, Christchurch, New Zealand, for facilities (R.K.), Dr. A. Willis, Research school of Chemistry, Australian National University, Canberra, Australia for data collection on compound **3**, Dr. C. K. Subramanian and B. R. Prasad, Department of Physics, for measurement of SHG activity, and Dr. G. N. Subbanna, Materials Research Centre, Indian Institute of Science, Bangalore, India, for particle size measurements.

Supporting Information Available: Lists of fractional atomic coordinates, bond distances and angles, and anisotropic thermal parameters for compounds **1**−**6** (47 pages); list of observed and calculated structure factors (75 pages). Ordering information is given on any current masthead page.

CM960123B